IEICE TRANS. FUNDAMENTALS, VOL. E75-A, NO. 7 JULY 1992

PAPER *Special Section on Multidimensional Signal Processing*

Property of Circular Convolution for Subband Image Coding

Hitoshi KIYA†, **Kiyoshi NISHIKAWA**† *and* **Masahiko SAGAWA**†, *Members*

SUMMARY One of the problems with subband image coding is the increase in image sizes caused by filtering. To solve this, it has been proposed to process the filtering by transforming input sequence into a periodic one. Then filtering is implemented by circular convolution. Although this technique solves the problem, there are very strong restrictions, i.e., limitation on the filter type and on the filter bank structure. In this paper, development of this technique is presented. Consequently, any type of linear phase FIR filter and any structure of filter bank can be used.

key words: *filter banks, image processing, subband image coding, high quality image coding*

1. Introduction

Subband image coding[1] (SBC) is one of the most efficient methods for high quality image coding at low bit rates. It is more attractive than the transform-based coding system, e.g., the DCT (Discrete Cosine Transform) based coding system[2], because it does not suffer from the blocking artifacts which afflict the latter. Recently, transform-based coding system without blocking effects have been developed[3],[4]. However, it is presented that we can treat them as a special case of the SBC[5]. Thus, concentrating on consideration of the SBC losts no generality of the theory.

The subband image coding system consists of a filter bank and a coding system. In designing the two dimensional filter banks, as the extension of one dimensional's, the main subjects are the removal of aliasing and the reduction of frequency distortion and phase distortion. In addition, the subband image coding system has an another requirement; the sum of the pixels in the subimages must be equal to the total number of pixels in the original image. However, it does not achieved, because the linear convolution of the spatially limited images expands the region of the support of the filtered image.

To avoid this problem, Smith et al. have proposed new techniques[6]-[8]. They have shown that the problem can be avoided if we apply the subband coding system by transforming the input sequence into a periodic one. They have proposed two methods for generating periodic sequence and have shown that there will be a difference in the efficiency of techniques depending on how to generate the periodic sequence. However, their techniques have restrictions as regards the filters consisting the filter bank and the structure of filter bank.

In this paper, we will modify their techniques and remove the restrictions. We propose general methods of generating periodic sequence. We show that it is possible to remove the restrictions by using our methods. Thus, any linear phase FIR filter can be used and any filter bank structure including the tree structure can be employed.

Noting that in this paper we only consider the separable systems. With separable filters the 2-D filtering can be implemented as a set of 1-D filtering operations. Filtering is first performed on each row and then on each column of the image. Therefore, the theory will be developed in terms of 1-D sequences and systems.

2. Conventional Methods

Here, we will review the subband image coding system and methods of Smith et al.

2. 1 Subband Image Coding System

A typical subband image coding system is shown in Fig. 1. It consists of a filter bank and a coding system. The filtering is needed in the analysis part and also in the synthesis part, namely in the decimation process and in the interpolation process, respectively.

The problem which we will consider is that the image size to be coded is expanded by the filtering. That is, the filtering in the decimation process increases the image size to be coded, i.e., the sum of the pixels of subimages $y_{nm}[m_1, m_2]$ become greater than that of input image $x[n_1, n_2]$.

This occurs because the size of the original image being finite. The linear convolution of the spatially limited images with filters expands the region of the support of the filtered image.

2. 2 Methods of Smith et al.

To solve this problem, Smith et al. have proposed

Manuscript received December 20, 1991.
Manuscript revised March 14, 1992.

† The authors are with Tokyo Metropolitan University, Hachioji-shi, 192-03 Japan.

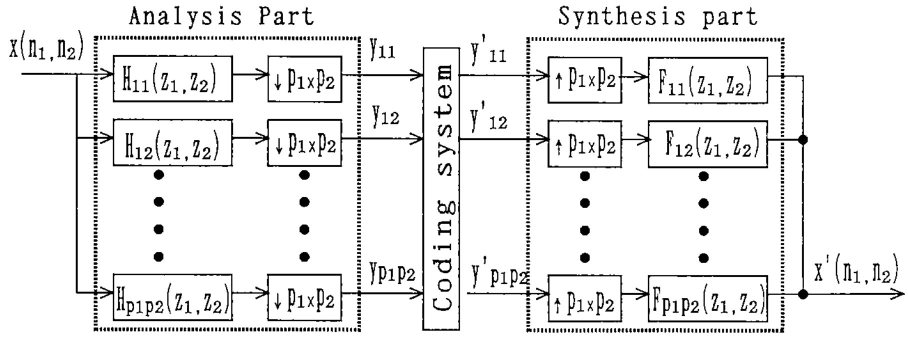

Fig. 1 A typical subband image coding system.

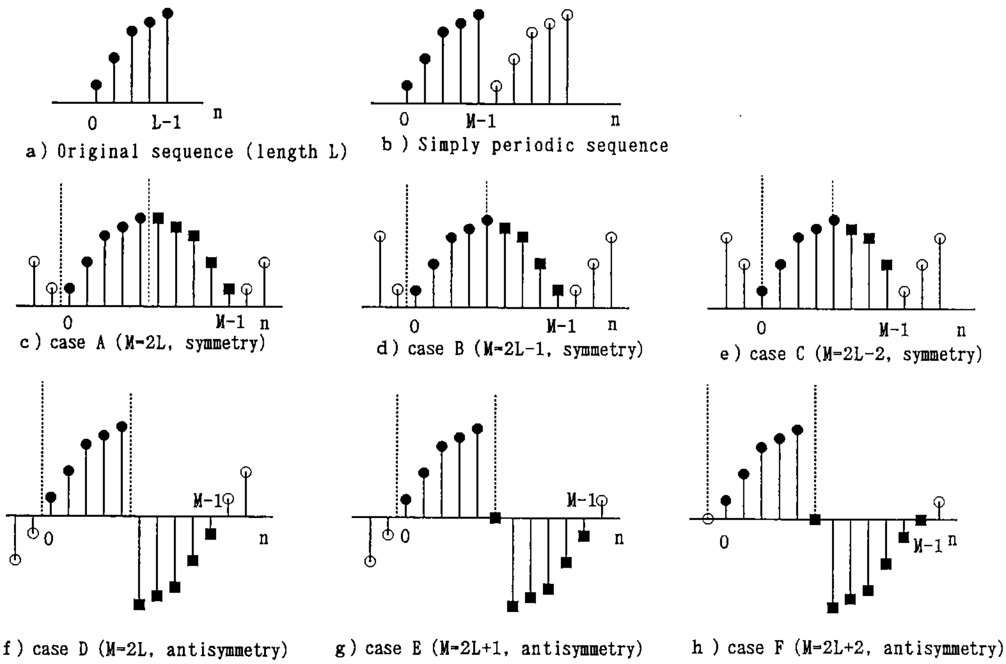

Fig. 2 Methods of generating periodic sequence.
(b) (c) Proposed by Smith et al.
(c)-(f) Our proposed method.

to apply the system by transforming the input sequence into a periodic one. Then the filtering is implemented by the circular convolution. Both the input sequence and output become periodic sequence of the same period, hence the problem of increasing image size is avoided. Nevertheless, it causes a time domain aliasing in $y_{mn}[m_1, m_2]$. However, if the filter bank is a perfect one, its transfer function will have a simple delay response. Therefore, even if the time domain aliasing occurs in the middle of the process, the output sequence of the filter bank $x'[n_1, n_2]$ will become delayed version of the input sequence $x[n_1, n_2]$.

They propose two methods of generating periodic sequence from the original one, as shown in Fig. 2(b) and (c). In Fig. 2(a), the original sequence is shown. They refer the method which uses the sequence of Fig. 2(b) as circular convolution method and the one which uses the sequence of Fig. 2(c) as symmetric extension method, respectively[6]. We regard them as same type methods in the point of view that they are both implemented by using circular convolution. Therefore, in the following consideration, we generally use the term circular convolution method for such methods which implemented by using circular convolution. They show that if we use the generated sequence of Fig. 2(c), the resulting image will be less affected by quantization noise than (b). Because of this, in the following, we will only consider the symmetrical periodic sequence. However, with their methods, there are restrictions on the filter type and on the structure of the filter bank. Namely, filters must have linear phase, the number of their impulse responses must be even and the filter bank structure must be the tree structure of two-band filter banks.

3. Proposed Methods

To remove these restrictions, we are proposing six methods[9], half of which for generating symmetric periodic sequences and the other half for anti-symmetric periodic sequences. We show them in Fig. 2(c)-(h). We refer three symmetric periodic sequences as cases A, B, and C, respectively and three anti-symmetric periodic sequences as cases D, E, and F. Note that case A sequence is one of those proposed by Smith et al.

In the following consideration, the frequency domain representation is superior than that of the time domain. Hence, we next consider to represent our proposed sequences in the frequency domain. The DFS (Discrete Fourier Series) of periodic sequence $\tilde{x}[n]$ is defined as

$$\tilde{X}[k]=\sum_{n=0}^{M-1}\tilde{x}[n]\,W_M^{kn}, \tag{1}$$

where M denotes the period of $\tilde{x}[n]$ and $W_M=\exp(-j2\pi/M)$. We use ~(tilde) to indicate the periodic sequence.

Using this definition, the proposed sequences can be expressed as below.

$$\tilde{X}_A[k]=W_M^{k(M-1)/2}\tilde{X}_A^*[k] \quad M:\text{even} \tag{2a}$$

$$\tilde{X}_B[k]=W_M^{k(M-1)/2}\tilde{X}_B^*[k] \quad M:\text{odd} \tag{2b}$$

$$\tilde{X}_C[k]=W_M^{kM/2}\tilde{X}_C^*[k] \quad M:\text{even} \tag{2c}$$

$$\tilde{X}_D[k]=j\tilde{X}_A[k] \tag{2d}$$

$$\tilde{X}_E[k]=j\tilde{X}_B[k] \tag{2e}$$

$$\tilde{X}_F[k]=j\tilde{X}_C[k], \tag{2f}$$

where M is the period of the generated sequence, $j=\sqrt{-1}$, $\tilde{X}_a^*[k]$ is purely real and subscript letter represents the type of the periodic sequence. Next, let us consider to shift the sequence $\tilde{x}[n]$, find the DFS of $\tilde{x}[n-s]$, where s is an arbitrary integer. By considering this, we can get a general expression of the periodic sequence in the frequency domain. From the property of DFS, Eq. (2) is reduced to

$$\tilde{X}_A[k]=W_M^{ks}W_M^{k(M-1)/2}\tilde{X}_A^*[k] \quad M:\text{even} \tag{3a}$$

$$\tilde{X}_B[k]=W_M^{ks}W_M^{k(M-1)/2}\tilde{X}_B^*[k] \quad M:\text{odd} \tag{3b}$$

$$\tilde{X}_C[k]=W_M^{ks}W_M^{kM/2}\tilde{X}_C^*[k] \quad M:\text{even} \tag{3c}$$

$$\tilde{X}_D[k]=j\tilde{X}_A[k] \tag{3d}$$

$$\tilde{X}_E[k]=j\tilde{X}_B[k] \tag{3e}$$

$$\tilde{X}_F[k]=j\tilde{X}_C[k]. \tag{3f}$$

In general, we can express these equations in a unified form. Namely,

$$\tilde{X}_a[k]=e^{jT}W_M^{kL}\tilde{X}_a^*[k]. \tag{4}$$

Table 1 Three parameters M, L, and T for each type of periodic sequence.

Sequence	M	L	T
A	even	Half Int.	$2n\pi$
B	odd	Int.	$2n\pi$
C	even	Int.	$2n\pi$
D	even	Half Int.	$2n\pi+\pi/2$
E	odd	Int.	$2n\pi+\pi/2$
F	even	Int.	$2n\pi+\pi/2$

n : integer
Int. : integer

In this equation, the type of periodic sequence is determined by three parameters, i.e., M, L and T. In Table 1, we tabulate them for each type of the periodic sequence.

Here, we show how to lead Eq. (2c).

$$\begin{aligned}\tilde{X}[k]&=\sum_{n=0}^{M-1}\tilde{x}[n]\,W_M^{kn}\\ &=\sum_{n=0}^{M/2-1}\tilde{x}[n]\,W_M^{kn}+\tilde{x}\left[\frac{M}{2}\right]W_M^{Mk/2}\\ &\quad+\sum_{n=M/2+1}^{M-1}\tilde{x}[n]\,W_M^{kn}\\ &=\sum_{n=0}^{M/2-1}\tilde{x}[n]\,W_M^{kn}+\sum_{m=1}^{M/2-1}\tilde{x}[M-m]\,W_M^{k(M-m)}\\ &\quad+\tilde{x}\left[\frac{M}{2}\right]W_M^{Mk/2},\end{aligned}$$

where we put $m=M-n$. Since $\tilde{x}[n]=\tilde{x}[M-n]$, for case C sequence,

$$\begin{aligned}\tilde{X}[k]&=\sum_{n=1}^{M/2-1}\tilde{x}[n][W_M^{kn}+W_M^{k(M-n)}]+\tilde{x}[0]\,W_M^{k0}\\ &\quad+\tilde{x}\left[\frac{M}{2}\right]W_M^{k(M/2)}\\ &=W_M^{Mk/2}\left[\sum_{n=1}^{M/2-1}\tilde{x}[n](W_M^{k(n-M/2)}+W_M^{k(M-n-M/2)})\right.\\ &\quad\left.+\tilde{x}[0]\,W_M^{-Mk/2}+\tilde{x}\left[\frac{M}{2}\right]\right]\\ &=W_M^{M/2-1}\left[\sum_{n=1}^{M/2-1}\tilde{x}[n](W_M^{k(n-M/2)}+W_M^{-k(n-M/2)})\right.\\ &\quad\left.+\tilde{x}[0]\,W_M^{Mk/2}+\tilde{x}\left[\frac{M}{2}\right]\right]\\ &=W_M^{Mk/2}\left[\sum_{n=1}^{M/2-1}2\,\tilde{x}[n]\cos\left(\frac{2}{M}k\left(n-\frac{M}{2}\right)\right)\right.\\ &\quad\left.+\tilde{x}[0]e^{-j\pi k}+\tilde{x}\left[\frac{M}{2}\right]\right]\\ &=W_M^{Mk/2}\tilde{X}^*[k].\end{aligned} \tag{5}$$

Other equations can be derived in the same manner.

4. Influence of Decimation

As described before, the problem of expanding image size is occurred in the decimation process. Therefore, we will study the influence of decimation on periodic sequence in the following. As shown in Fig. 3, the decimator consists of two components, namely a filter and a down-sampler, and their respective influence on periodic sequence will be considered.

We refer the input sequence of the filter as $\tilde{x}[n]$, the output of the filter as $\tilde{g}[n]$ and $\tilde{y}[n]$ as the output of the down-sampler. Let P denotes integer decimation factor. To satisfy the purpose of assuming the periodic input sequences, i.e., to avoid the increase in the number of independent pixels by the filtering, the following two conditions must be fulfilled.
(i) The period M of $\tilde{x}[n]$ must be the integer multiple of P. Because the period of $\tilde{y}[m]$ is M/P and it must be integer
(ii) $\tilde{y}[m]$ must be a symmetrical sequence when $\tilde{x}[n]$ is a symmetrical one. Otherwise, the number of independent values increases after decimation process.

4.1 Filtering and Periodic Sequence

4.1.1 Influence of the Filtering

First, let us consider the influence of the filtering on periodic sequence. In the following, we will only consider the systems consisting of linear phase FIR (LPFIR) filters. The LPFIR filters can be classified into four cases according to their impulse responses, and are shown in Fig. 4. When the symmetrical periodic sequence $\tilde{x}[n]$ is filtered with the LPFIR filters,

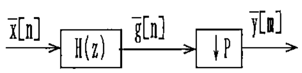

Fig. 3 A P-fold decimator.

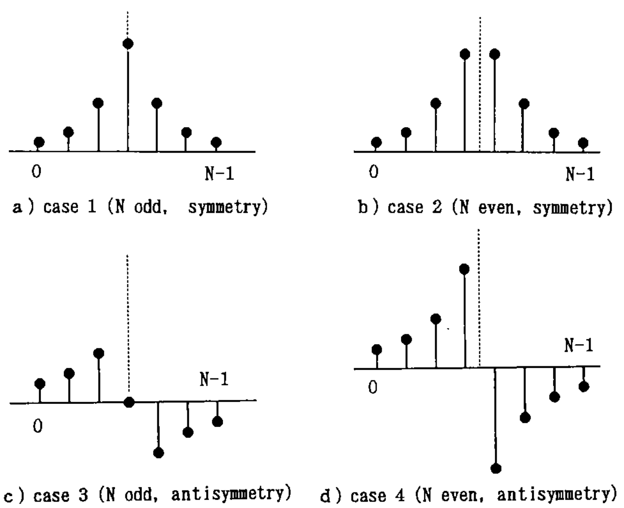

Fig. 4 Types of linear phase FIR filters.

then the output sequence $\tilde{g}[n]$ will also become a symmetrical periodic sequence. Moreover, the period of $\tilde{x}[n]$ and $\tilde{g}[n]$ will become the same one. Nevertheless, the filtering may change the periodic case of the sequence. In Table 2, the periodic case of $\tilde{g}[n]$, the output sequence of the filter, is shown. In this Table, the relations marked by * (asterisk) are pointed out by Smith et al. Therefore, Table 2 shows more general relations including those pointed out by Smith et al.

4.1.2 Theoretical Consideration

Using frequency domain representation, the relations shown in Table 2 can be explained as follows. The frequency responses of the LPFIR filters can be expressed as Ref.(10).

$$H_1(e^{j\omega}) = e^{-j\omega\frac{N-1}{2}} H_1^*(e^{j\omega}) \qquad N\text{: odd} \tag{6a}$$

$$H_2(e^{j\omega}) = e^{-j\omega\frac{N-1}{2}} H_2^*(e^{j\omega}) \qquad N\text{: even} \tag{6b}$$

$$H_3(e^{j\omega}) = jH_1(e^{j\omega}) \tag{6c}$$

$$H_4(e^{j\omega}) = jH_2(e^{j\omega}), \tag{6d}$$

where $H_n^*(e^{j\omega})$ is purely real, and N denotes filter length. These equations can be unified in the next form. That is,

$$H_n(e^{j\omega}) = e^{jC} e^{-j\omega B} H_n^*(e^{j\omega}), \tag{7}$$

where B and C are two parameters identifying the type

Table 2 Periodic case of the output sequence of the filter.

				FILTER TYPE			
				Symmetry		Anti-symmetry	
				odd	even	odd	even
				1	2	3	4
Sequence type	Symmetry	even I	A	A	C*	D	F*
		odd	B	B	B	E	E
		even II	C	C	A	F	D
	Anti-Symmetry	even I	D	D	F	A	C
		odd	E	E	E	B	B
		even II	F	F	D	C	A

* pointed out by Smith et al.

Table 3 Two parameters B and C for each type of linear phase FIR filters.

Filter	B	C
1	Int.	$2n\pi$
2	Half Int.	$2n\pi$
3	Int.	$2n\pi+\pi/2$
4	Half Int.	$2n\pi+\pi/2$

n : integer
Int. : integer

of the LPFIR filter. In Table 3, we tabulate B and C for each type.

Using Eqs. (4) and (7), we can derive the relations shown in Table 2. Let us denote DFS of $\tilde{g}[n]$ as $\tilde{G}[k]$ and is expressed as,

$$\begin{aligned}\tilde{G}[k] &= H(e^{j\omega})\tilde{X}[k] \\ &= e^{jC}e^{-j\omega B}H^*(e^{j\omega})e^{jT}W_M^{kL}\tilde{X}^*[k] \\ &= e^{jC}e^{-j\omega_k B}H^*(e^{j\omega_k})e^{jT}W_M^{kL}\tilde{X}^*[k] \\ &= e^{jC}e^{-j\omega_k B}e^{jT}W_M^{kL}\tilde{G}^*[k], \qquad (8)\end{aligned}$$

where $\omega_k = 2\pi k/M$ and $\tilde{G}^*[k] = H^*(e^{j\omega_k})\tilde{X}^*[k]$. Therefore, we can obtain

$$\tilde{G}[k] = e^{j(C+T)}W_M^{k(B+L)}\tilde{G}^*[k]. \qquad (9)$$

For example, let us consider the case that $\tilde{x}[n]$ is a case A sequence and $h[n]$ is a case 2 filter. Then $C+T=0$, $B+L$ is an integer and M is even. It is known from Table 1 that the resulting sequence $\tilde{g}[n]$ becomes a periodic sequence of case C. We show another example. When we consider the case that $\tilde{x}[n]$ is case F and $h[n]$ is case 4, then $C+T=\pi$, $B+L$ is a half integer and M is even. Therefore, the resulting sequence becomes a case A sequence.

4.2 Down-Sampling and Periodic Sequences

Next, we will consider the influence of the down-sampling on periodic sequences. That is, we will consider the periodic type of $\tilde{y}[n]$ which is generated by down-sampling $\tilde{g}[n]$.

4.2.1 The Influence of Down-Sampling

When the decimation ratio is P, then $\tilde{y}[m]$ is formed by saving only every Pth sample of the filtered output $\tilde{g}[n]$. It is noted that even if $\tilde{g}[n]$ has symmetry, $\tilde{y}[m]$ may not have symmetry. In another words, down-sampling affects the symmetry of the sequence, i.e., the symmetrical sequence may lose its symmetry after down-sampled. In that case, the number of independent values will be increased. Hence, the condition (ii) must be required. Moreover, even if the symmetry holds, the type of the down-sampled sequence varies depending on the timing of decimation. For example, we show this in Fig. 5 when $\tilde{g}[n]$ is a case C. As shown in the figure, we can distinguish two kinds of decimation. Let us define Decimation I as the decimation which leaves the value corresponding to the center of symmetry, and Decimation II as the one which does not leave the value corresponding to the center of symmetry.

In Table 4, we have tabulated the relations of the sequence types, P and M. It is known from this table that the sequences which will have symmetry after down-sampled are limited. Therefore, the sequence

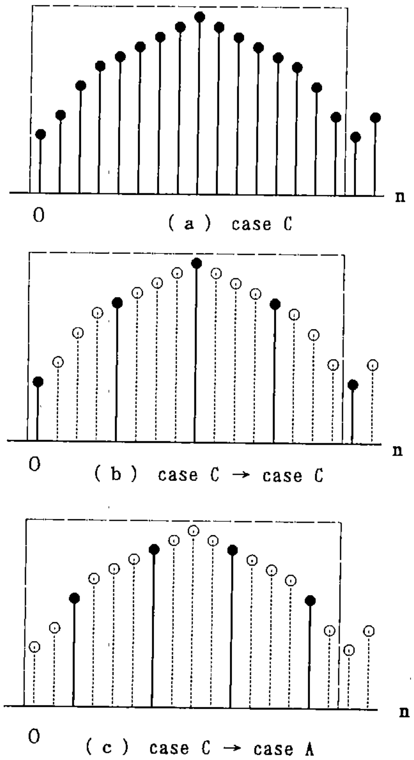

Fig. 5 Influence of the timing of decimation.
(a) Original sequence.
(b) Decimated sequence with decimation I.
(c) Decimated sequence with decimation II.

Table 4 Periodic case of the decimated sequence.

Sequence type		P:even, M: even multiple of P	P:even, M: odd multiple of P	P: odd, M: even multiple of P	P: odd, M: odd multiple of P
A	Dec I	–	–	–	×
A	Dec II	–	–	A	×
B	Dec I	×	×	×	B
B	Dec II	×	×	×	–
C	Dec I	C	B	C	–
C	Dec II	A*	B	–	–
D	Dec I	–	–	–	×
D	Dec II	–	–	D	×
E	Dec I	×	×	×	E
E	Dec II	×	×	×	–
F	Dec I	F	E	F	–
F	Dec II	D*	E	–	–

Dec I : decimated with decimation I
Dec II : decimated with decimation II
× : conflict with condition(i) (see sec. 4)
– : conflict with condition(ii)
* pointed out by Smith et al.
P : decimation ratio
M : period of the input sequence of the decimator

type must be selected according to Table 4 to satisfy the above two conditions.

In special case of $P=2$, for example, it is known from Table 4 that the filtered sequence $\tilde{g}[n]$ which satisfy the above conditions are only cases C and F. Therefore, with methods of Smith et al. the type of LPFIR filter must be cases 2 or 4 because they use only case A sequence as input $\tilde{x}[n]$. In addition, the filter bank structure must be the tree structure of two-band filter banks, because they only consider the case of $P=2$. In Table 4, the relations they have pointed out are marked with * (asterisk). The filter bank satisfying these restrictions is only the classical Quadrature Mirror Filter (QMF) banks(11),(12).

On the other hand, known from Table 4, we can use LPFIR filters of cases 1 and 3 if we take case C sequence as $\tilde{x}[n]$. Hence, our methods will make it possible to use a filter bank consisting of any LPFIR filters, such as the perfect QMF banks(13),(14).

It is noted that we can select either of symmetry or anti-symmetry sequence as a input sequence of analysis bank. The selection must be done according to the statistical property of the original signal. DCT can be regarded as a special case of the circular convolution method using symmetry sequence, and DST (Discrete Sine Transform) as the one using anti-symmetry sequence. Therefore, when processing the signals such as image or speech signal, we should select symmetry sequence owing to the same reason DCT is superior than DST when we process such signals.

4.2.2 Consideration on Table 4

Here, we derive the relations shown in Table 4. To see this, we first formulate the relations between $\tilde{g}[n]$ and $\tilde{y}[m]$. Let M denotes the period of $\tilde{x}[n]$ and P denotes integer decimation factor, then they have a relation $M=M'P$, where M' is the period of decimated sequence $\tilde{y}[m]$.

We define the sequence $\tilde{g}'[n]$ as

$$\tilde{g}'[n]=\begin{cases}\tilde{g}[n-s] & n=0, P, 2P, \cdots \\ 0 & \text{otherwise,}\end{cases} \tag{10}$$

for later convenience. Where s represents a shift value which determines the timing of decimation. A convenient and useful representation of $\tilde{g}'[n]$ is known as(15)

$$\tilde{g}'[n]=\tilde{g}[n-s]\frac{1}{P}\sum_{l=0}^{P-1}e^{j2\pi ln/P}. \tag{11}$$

From this, we get

$$\tilde{y}[m]=\tilde{g}'[Pm]=\tilde{g}[Pm-s]. \tag{12}$$

Now, we write the DFS of $\tilde{y}[m]$ as

$$\begin{aligned}\tilde{Y}[k]&=\sum_{m=0}^{M'-1}\tilde{y}[m]\,W_{M'}^{km}\\
&=\sum_{m=0}^{M'-1}\tilde{g}'[Pm]\,W_{M'}^{km}\\
&=\sum_{n=0}^{M-1}\tilde{g}'[Pn]\,W_{M'}^{kn/P}\\
&=\sum_{n=0}^{M-1}\tilde{g}[n-s]\sum_{l=0}^{P-1}\exp\left(\frac{j2\pi ln}{P}\right)W_{M'}^{kn/P}\\
&=\frac{1}{P}\sum_{l=0}^{P-1}\sum_{n=0}^{M-1}\tilde{g}[n-s]\exp\left(\frac{j2\pi ln}{P}\right)W_{M'}^{kn/P}\\
&=\frac{1}{P}\sum_{l=0}^{P-1}\sum_{n=0}^{M-1}\tilde{g}[n-s]\exp\left(j\frac{2\pi}{M}n\left(k-\frac{Ml}{P}\right)\right)\\
&=\frac{1}{P}\sum_{l=0}^{P-1}\exp\left(-j\frac{2\pi}{M}s\left(k-\frac{Ml}{P}\right)\right)\\
&\quad\cdot\tilde{G}\left[k-\frac{Ml}{P}\right]\\
&=\frac{1}{P}\sum_{l=0}^{P-1}W_M^{s(k-Ml/P)}\tilde{G}\left[k-\frac{Ml}{P}\right]\end{aligned} \tag{13}$$

where $\tilde{G}[k]$ is the DFS of $\tilde{g}[n]$.

Using Eq. (13), we will derive the relations shown in Table 4 as follows. When $\tilde{g}[n]$ is a periodic sequence of case A then we get by substituting (2a) into (13),

$$\begin{aligned}\tilde{Y}[k]&=\frac{1}{P}\sum_{m=0}^{P-1}W_M^{s(k-Mm/P)}\tilde{G}\left[k-\frac{Mm}{P}\right]\\
&=\frac{1}{P}\sum_{m=0}^{P-1}W_M^{s(k-Mm/P)}\,W_M^{1/2(M-1)(k-Mm/P)}\\
&\quad\cdot\tilde{G}^*\left[k-\frac{Mm}{P}\right]\\
&=\frac{1}{P}W_M^{(s+(M-1)/2)k}\\
&\quad\cdot\sum_{m=0}^{P-1}W_M^{-Mm(s+(M-1)/2)(1/P)}\tilde{G}^*\left[k-\frac{Mm}{P}\right].\end{aligned}$$

Because $M'=M/P$,

$$\begin{aligned}&\tilde{Y}[k]\\
&=\frac{1}{P}W_{M'}^{(s+(PM'-1)/2)(k/P)}\\
&\quad\cdot\sum_{m=0}^{P-1}\exp\left[j\pi m\left(M'+\frac{2s-1}{P}\right)\right]\tilde{G}^*[k-M'm]\\
&=\frac{1}{P}W_{M'}^{(M'/2+(2s-1)/2P)k}\\
&\quad\cdot\sum_{m=0}^{P-1}\exp\left[j\pi m\left(M'+\frac{2s-1}{P}\right)\right]\tilde{G}^*[k-M'm]\\
&=\frac{1}{P}W_{M'}^{(M'+b)k/2}\sum_{m=0}^{P-1}\exp\left[j\pi m(M'+b)\right]\\
&\quad\cdot\tilde{G}^*[k-M'm]\end{aligned} \tag{14}$$

where we put $(2s-1)/P=b$. Here, consider about to express Eq. (14) in the form of Eq. (3). For that, in Eq. (14), exponential term in summation must be real.

It requires M and $(2s-1)$ must be integer multiple of P, hence b must be integer. Consequently, each of next two variables

$$M'=\frac{M}{P}, \tag{15a}$$

$$s=\frac{bP+1}{2} \tag{15b}$$

must be integer. From Eq. (15), the relation in Table 4 can be derived. That is, from Eq. (15b), $(bP+1)$ must be integer multiple of 2, or bP required to be odd, therefore decimation ratio P must be odd. For case A sequence, the period M is even, hence M' becomes even. Because the case A sequence does not have a value which corresponding to the center of symmetry, only decimation II can be available.

When $\tilde{g}[n]$ is case B, the condition for M and s are also given by Eq. (15).

Next, let us consider the case when $\tilde{g}[n]$ is a sequence of case C. Then by substituting (2c) into (13) we get

$$\begin{aligned}\tilde{Y}[k]&=\frac{1}{P}\sum_{m=0}^{P-1} W_M^{s(k-Mm/P)}\tilde{G}\left[k-\frac{Mm}{P}\right]\\&=\frac{1}{P}\sum_{m=0}^{P-1} W_M^{s(k-Mm/P)}\, W_M^{M(k-Mm/P)/2}\\&\quad\cdot\tilde{G}^*\left[k-\frac{Mm}{P}\right]\\&=\frac{1}{P}W_M^{k(s+M/2)}\sum_{m=0}^{P-1} W_M^{-Mm(s+M/2)/P}\\&\quad\cdot\tilde{G}^*\left[k-\frac{Mm}{P}\right]\\&=\frac{1}{P}W_{M'}^{(s+PM'/2)(k/P)}\sum_{m=0}^{P-1}\exp\left[j\pi m\left(M'+\frac{2s}{P}\right)\right]\\&\quad\cdot\tilde{G}^*[k-M'm]\\&=\frac{1}{P}W_{M'}^{(M'/2+2s/2P)k}\sum_{m=0}^{P-1}\exp\left[j\pi m\left(M'+\frac{2s}{P}\right)\right]\\&\quad\cdot\tilde{G}^*[k-M'm].\end{aligned}$$

By putting $2s/P=b$, we get

$$\begin{aligned}\tilde{Y}[k]&=\frac{1}{P}W_{M'}^{(M'+b)k/2}\sum_{m=0}^{P-1}\exp\left[j\pi m(M'+b)\right]\\&\quad\cdot\tilde{G}^*[k-M'm].\end{aligned} \tag{16}$$

Again, we require each of next two variables

$$M'=\frac{M}{P}, \tag{17a}$$

$$s=\frac{bP}{2} \tag{17b}$$

must be integer. From Eq. (17), the relation in Table 4 can be derived.

The same results for sequences of cases D to F are derived in the same way.

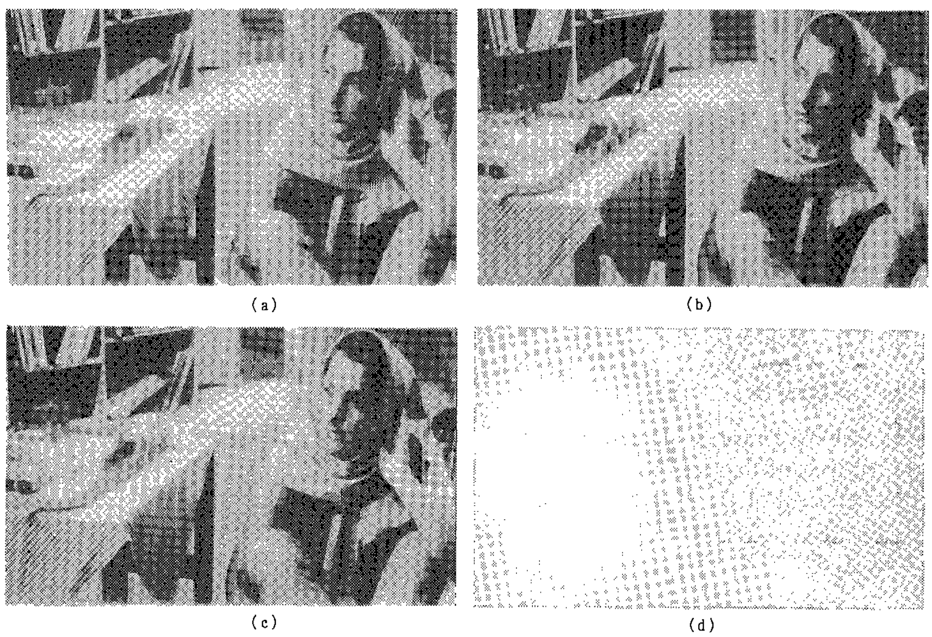

Fig. 6 Examples of original and several coded images at 8-bit.
(a) Original. Enclosed areas (256×256) have been processed.
(b) Method based on symmetric data.
(c) Method based on non-symmetric data.
(d) Difference between (b) and (c).

5. Simulation Results

As an example, computer simulations were carried out. A comparison between the method based on non-symmetric data (Fig. 2(b)) and the method on symmetrical data was made. Fig. 6 provides original and reconstructed images.

These comparisons are based on simulations of uniform 16-band subband image coders for 256×256 images. We use the tree structure of the two-band symmetric short kernel filters (SSKF)[13], which belongs to case-1 type, as 1-D filter bank. Its transfer functions are

$$H_0[z]=\frac{1}{8}(-1+2z^{-1}+6z^{-2}+2z^{-3}-z^{-4}) \quad (18)$$

$$H_1[z]=\frac{1}{2}(1-2z^{-1}+z^{-2}) \quad (19)$$

which have odd length, or case-1 LPFIR filters. Hence, the symmetrical periodic sequence cannot be applied with Smith's methods. From Table 4, it is known, under the above conditions, the filtered sequence $g[n]$ must be case C or case F. Then, known from Table 2, the input sequence must be case C or case F. In this simulation, the input image was transformed into a case C sequence because of the reason mentioned in Sect. 4. 2.

The input image was first divided into 16-band by applying 1-D filters along their respective rows and columns. For the lowest band 8-bit length quantization is applied, and the higher bands are abandoned. Finally, the decomposed data are synthesized.

From the figure, it is verified that data distortion is not negligible near the edge of the image especially in the method based on non-symmetric data.

6. Conclusion

In this paper, we have developed a technique for high quality subband image coding with low bit rates proposed by Smith et al. We have proposed six methods of generating symmetrical periodic sequence and investigated its behavior in the QMF analysis/synthesis system. Especially, the influence of the decimation process on periodic sequence is considered in detail.

In that, we used the frequency domain representations so that the theory can be clearly developed. We have led the conditions used in the general structure of analysis/synthesis system. Therefore, the restrictions on the filter type and on the filter bank structure can be removed.

References

(1) Woods J. W. and O'Neil S. D.: "Subband coding of images", IEEE Trans. Acoust., Speech, Signal Processing, **ASSP-34**, pp. 1278-1288 (Oct. 1986).

(2) Ahmed N., Natarajan T. and Rao K. R.: "Discrete cosine transform", IEEE Trans. Comput., **23**, pp. 90-93 (Jan. 1974).

(3) Malvar H. S. and Staelin D. H.: "The LOT: Transform coding without blocking effects", IEEE Trans. Acoust., Speech, Signal Processing, **37**, pp. 553-559 (April 1989).

(4) Lookabaugh T. D. and Perkins M. G.: "Application of the Princen-Bradley filter bank to speech and image compression", IEEE Trans. Acoust., Speech, Signal Processing, **38**, pp. 1914-1926 (Nov. 1990).

(5) Vetterli M. and Le Gall D.: "Perfect reconstruction FIR filter banks: some properties and factorizations", IEEE Trans. Acoust., Speech, Signal Processing, **37**, pp. 1057-1071 (July 1989).

(6) Smith M. J. T. and Eddins S. L.: "Analysis/Synthesis Techniques for Subband Image Coding", IEEE Trans. Acoust., Speech, Signal Processing, **ASSP-38**, pp. 1446-1456 (Aug. 1990).

(7) Kim C. S., Bruder J., Smith M. J. T. and Mersereau R. M.: "Subband coding of color images using finite state vector quantization", Proc. Int. Conf. Acoust., Speech, Signal Processing, pp. 753-756 (1988).

(8) Smith M. J. T. and Eddins S. L.: "Subband coding images with octave band tree structures", Proc. Int. Conf. Acoust., Speech, Signal Processing, pp. 1378-1381 (April 1987).

(9) Nishikawa K., Kiya H. and Sagawa M.: "Property of circular convolution for subband image coding", Proc. Int. Conf. Acoust., Speech, Signal Processing (March 1992).

(10) Rabiner L. R. and Gold B.: "Theory and Application of Digital Signal Processing", Prentice-Hall, Englewood Cliffs, NJ (1975).

(11) Croisier A., Esteban D. and Galand C.: "Perfect channel splitting by use of interpolation/decimation/tree decomposition techniques", Proc. IEEE Int. Conf. Inform. Sci. Syst., pp. 443-446 (1976).

(12) Esteban D. and Galand C.: "Application of quadrature mirror filters to splitband voice coding schemes", Proc. Int. Conf. Acoust., Speech, Signal Processing, pp. 191-195 (1977).

(13) Le Gall D. and Tabatabai A.: "Subband coding of digital images using symmetric short kernel filters and arithmetic coding techniques", Proc. Int. Conf. Acoust., Speech, Signal Processing, pp. 761-764 (April 1988).

(14) Kiya H., Yae M. and Iwahashi M.: "A linear phase two-channel filter bank allowing perfect reconstruction", Proc. Int. Symp. Circuits Syst. (May 1992).

(15) Crochiere R. E. and Rabiner L. R.: "Multirate Digital Signal Processing", Sec. 2.3, Prentice-Hall, Englewood Cliffs, NJ (1983).

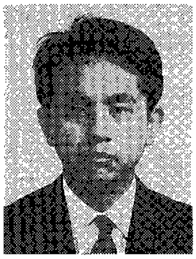

Hitoshi Kiya was born in Yamagata, Japan on November 16, 1957. He received the B.E. and M.E. degrees in electrical engineering from Nagaoka University of Technology, and the D.E. degree in electrical engineering from Tokyo Metropolitan University in 1980, 1982 and 1987, respectively. Since 1982, he has been with Tokyo Metropolitan University, as an Assistant Professor. His current research interests include multirate digital processing, image processing and adaptive signal processing. He is a co-author of three books which are "The Fast Fourier Transform Algorithm", "Digital Control System Analysis and Design", and "The Fast Fourier Transform and Its Applications". He is a member of IEEE CAS and ASSP Society, and a member of the institute of image electronics engineers of Japan.

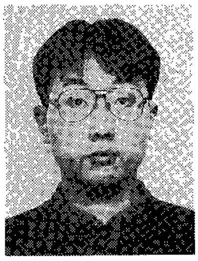

Kiyoshi Nishikawa was born in Tokyo, Japan on December 12, 1966. He received the B.E. and the M.E. degrees in electrical engineering from Tokyo Metropolitan University in 1990 and 1992, respectively. He is now with Nippon Steel Co. His research interest includes the digital image processing.

Masahiko Sagawa received the B.E., M.E. and D.E. degrees in electrical engineering from Tokyo Institute of Technology, Tokyo, Japan, in 1957, 1959 and 1964, respectively. He is currently a Professor at Tokyo Metropolitan University. His research interest include digital signal processing. He is a member of the IEEE.